Effect of Strongly-Coupled Vibration-Cavity Polaritons on the Bulk Vibrational States within a Wavelength-Scale Cavity

Justin Erwin, Madeline Smotzer, and James V. Coe*

.

The Ohio-State University Department of Chemistry and Biochemistry, 100 West 18th Avenue, Columbus OH 43210-1173.

Corresponding Author

*Email: coe.1@osu.edu

ABSTRACT. A Rabi splitting of 43.0 ± 1.0 cm^{-1} (95 % conf.) was determined for the interaction of the CD_3 deformation, the strongest fundamental vibration of the liquid $CD_3C{\equiv}N$ molecule, and fringe modes of a parallel plate Fabry-Pérot cavity containing this liquid. Note that vibration-cavity polaritons are also called dressed states, hybrid or mixed states. Since the experimental configuration has many orders of magnitude more vibrational oscillators than photons, vibrational oscillators not in dressed states far outnumber the dressed states. This work is distinguished from related vibration-cavity work by a method to extract the position, width, phase, and intensity of bulk vibrational signals including reconstruction of the position of the

fringe without vibrational contributions. It reveals how the bulk vibrational oscillators are changed by interaction within the cavity even though they are not in dressed states. While the dressed states are obvious targets for manipulation of chemical response, it is interesting to consider whether the lesser but more prevalent changes of the bulk vibrations can also be used to change chemical response.

TOC GRAPHICS

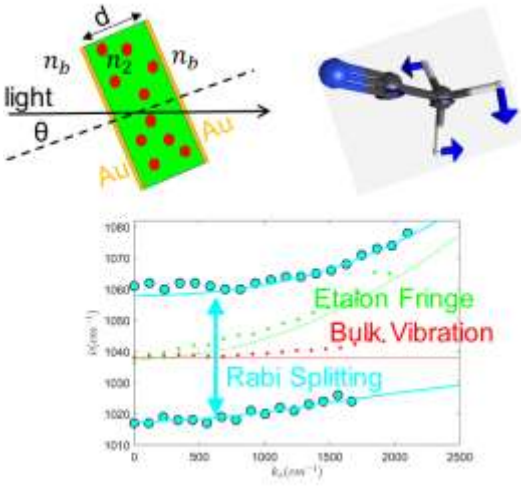

KEYWORDS. Cavity-vibration mixed states, infrared microcavity, etalon, mixed states of light and matter, wavelength-scale Fabry-Pérot.

INTRODUCTION

Recent experimental studies at the Naval Research Lab[1-2], in Strasbourg[3-7], and Israel[8-10] reveal that simple experimental arrangements enable definitive measurements on Rabi splittings of vibration-cavity mixed states in condensed phase systems. A standard infrared (IR) liquid cell with a micrometer-scale spacer has its ZnSe windows coated with 10 nm of Au producing mirrors and a wavelength-scale parallel plate etalon or Fabry-Pérot cavity which interacts with a

bulk-scale number of vibrational oscillators by means of a standard Fourier Transform Infrared Spectrometer (FTIR). Fringes are tuned into resonance with vibrations by tuning the angle θ of the cavity to the incident beam (see the top left insert of Figure 1). While the literature of cavity-vibration Rabi splittings is growing[1-7, 9-16], early successful vibrations tended to be triple bond and coupled double bond systems like -N=C=O, C=O=C, N=N=N, O=C=O, C=O, C≡N and C≡O (including these as ligands) since these are strong and local vibrations with large dipole derivatives and isolated from solvent density of states.

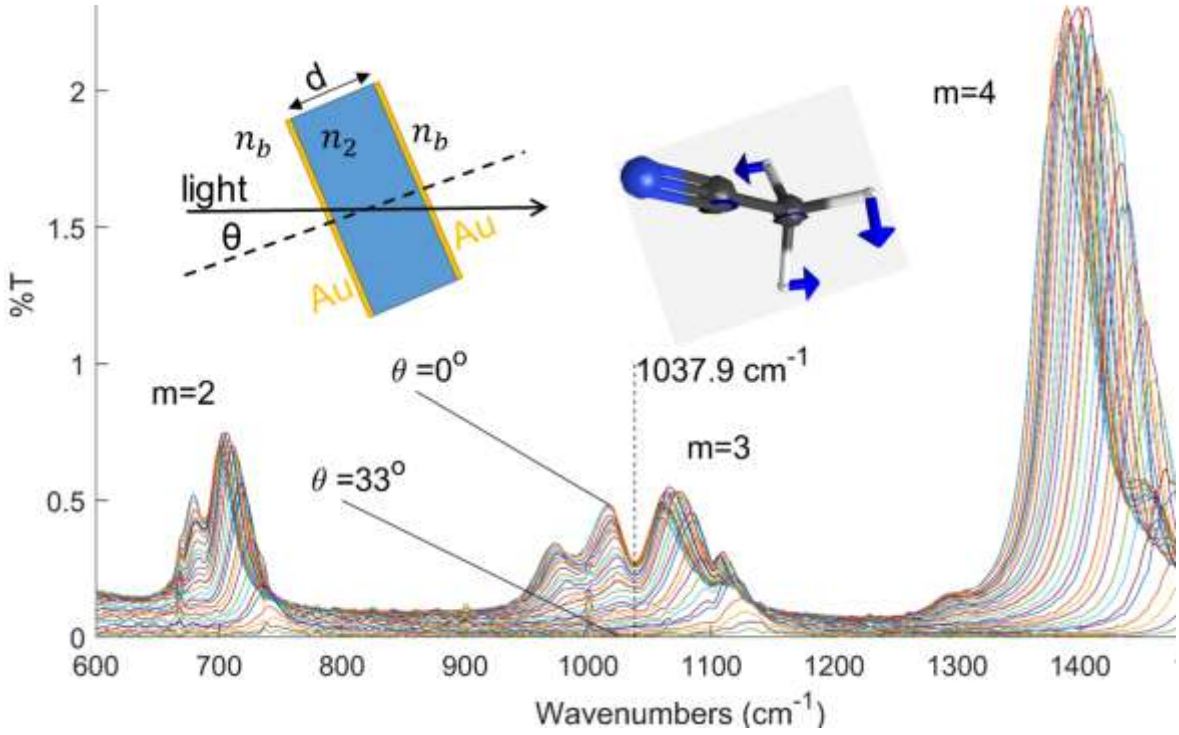

Figure 1. IR transmission spectra of ~12 μm spaced etalon filled with d3-acetonitrile with $\theta = 0^o$ *to* 33^o (1° steps). The $m = 3$ fringe tunes through the strong vibration at 1037.9 cm^{-1}.

The expression for the Rabi splitting ($\hbar\Omega_{1,0}$) is discussed in reviews[17-18] and derives from cavity quantum electrodynamics[19] in which we replace the electronic atom transition with a fundamental molecular vibrational transition, i.e. $\hbar\Omega_{1,0} = 2\overrightarrow{D_{1,0}} \cdot \overrightarrow{E_{cav}} = 2\gamma D_{1,0} E_{cav}$, where $D_{1,0}$ is the matrix element of the fundamental vibrational transition from the ground state to the first

excited state of a chosen vibration, E_{cav} is the rms field amplitude of light in the cavity, and γ varies with the orientation averaging associated with particular polarization and experimental arrangements. We added the factor of two for consistency with the coupling constant of matrix formulations, i.e. the Rabi splitting is twice the coupling constant in the absence of other complications like resonance widths. The Rabi splitting in the harmonic approximation for a vibration and cavity fringe of equal energy and for a large number of vibrational oscillators, N, is

$$E_{Rabi\ 1,0} = \hbar\Omega_{1,0}\sqrt{N} = \gamma\left[\left(\frac{\partial p}{\partial Q}\right)_0 \frac{1}{\sqrt{\mu}}\right]\frac{\hbar}{\sqrt{\epsilon}}\sqrt{\frac{N}{V}} \quad , \qquad (1)$$

where μ is the reduced mass of the vibrational oscillator, $\sqrt{\epsilon}$ is the index of refraction of the cavity dielectric, V is the illuminated volume of the cavity, and the subscript of $E_{Rabi\ 1,0}$ where the part of the subscript 1,0 indicates that the expression is only valid for a transition from the ground state to a fundamental mode of the chosen vibration. Note the dependence on the square root of concentration, $\sqrt{N/V}$, and $\left(\frac{\partial p}{\partial Q}\right)_0 \frac{1}{\sqrt{\mu}}$, which is the dipole derivative in reduced mass-weighted coordinates. The *ab intio* program Gaussian[20] calculates the Cartesian components of $\left(\frac{\partial p}{\partial Q}\right)_0 \frac{1}{\sqrt{\mu}}$ for a molecule and uses the sum of the squares of Cartesian components[21-22] as the "IR intensity" for each vibration in units of km/mol [$1\ D^2/(\text{Å}^2 amu)$ =42.2561 km/mol]. Rabi splitting work uses the mass-weighted dipole derivatives without squaring them, i.e. the square root of the IR intensities provided by Gaussian or other ab initio programs. The Rabi splitting for a fundamental vibrational transition in cm^{-1} units is

$$\tilde{\nu}_{1,0}(cm^{-1}) = \gamma\frac{2.247x10^{-10}}{n_{cav}} g\sqrt{I\left(\frac{km}{mol}\right)}\sqrt{\frac{N}{V}\left(\frac{molecules}{cm^3}\right)} \quad , \qquad (2)$$

where n_{cav} is the index of refraction of the cavity contents, g is the degeneracy of the vibration, N/V is the number density of molecules calculated from the density and molecular weight, and I

is the IR intensity as calculated by ab initio methods (units of km/mol). Most common absolute IR absorption arrangements using a narrow beam of light have an orientation factor of $\gamma = 1/3$ which is $\langle(cos\theta)^2\rangle$, the average value of the square of the dot product between the light's electric field and dipole derivative on a unit sphere. Since a Rabi splitting has the same interaction except for not being squared, we have chosen $\gamma = 1/2$ which is $\langle|cos\theta|\rangle$, the average value of the dot product interaction angle ignoring phase. The subject vibration of this work is the CD_3 deformation of fully deuterated acetonitrile ($CD_3C{\equiv}N$) which was calculated at the MP2/cc-pVDZ level of theory to have $\tilde{\nu} = 1060\ cm^{-1}$, $\mu = 2.117\ Daltons$, $k = 1.403\ mDyne/$Å, and "IR Inten"$= 4.766\ km/mol$. Use of the dipole derivative with $\gamma = 0.5$, $g = 2, n_2 = 1.368$, $\rho = 0.844\ g/cm^3$, $MW = 44.07 g/mol$, predicts a Rabi splitting of $38.7\ cm^{-1}$ with gas phase values which is near to the value measured for the liquid in this work.

EXPERIMENTAL

A Harrick liquid IR cell (DLC-S13, 13 mm diam. ZnSe windows, Swagelock fittings) was acquired for this experiment. Mirrors were made by evaporating a 2 nm coating of Ti as an adhesion layer, followed by 10 nm of Au on the ZnSe ($\lambda/4$, Crystan UK) windows at the OSU Nanotech West Lab. A drop of d_3-acetonitrile ($CD_3C{\equiv}N$, Sigma, Lot # 112F-0541, $MW = 44.07\ g/mol$, $n_2 = 1.341$ in vis., $\rho = 0.844 \frac{g}{cm^3}$ at 25 C, 99%) was placed on one mirror with a nominally 12 μm PTFE spacer and then the whole assembly was hand-tightened leaving a microcell filled with liquid. It appears easier to start with a filled cell and evacuate it, rather than the other way around. IR spectra were recorded in a Perkin Elmer Spectrum 100 FTIR (4 cm^{-1} resolution, 1 cm^{-1} steps, from 500-6000 cm^{-1}, 128 scans) at 1^o steps from $\theta = 0^o\ to\ 33^o$ (Edmund Optics #53-026 rotary mount) as shown in Figure 1. The vibration with the strongest

dipole derivative is the CD_3 asymmetric deformation at ~1037.9 cm^{-1} (the C≡N stretch seems stronger because it is so narrow). The spectra are uncorrected for reduced transmission with higher angle θ. Note how the $m = 3$ fringe tunes through the 1037.9 cm^{-1} vibration. After the cavity experiment, the liquid cell was constructed without mirrors, just ZnSe windows and the same spacer, in order to provide a calibrating standard IR absorption spectrum.

RESULTS

A set of transmission maximum positions was extracted for each spectrum of angle θ using the data in Figure 1 with a Matlab template (Matlab function "findpeaks" with settings such as "MinPeakDistance" = 10, "MinPeakHeight" = 0.1, and "MinPeakProminence" = ~0.06). The transmission maxima are plotted using cyan symbols vs k_x in Figure 2 where $k_x = 2\pi\tilde{\nu}sin\theta$. Noticing that the fringe labeled $m = 4$ in Figure 1 has no strong vibrational peaks, data was extracted from the regions of fringes $m = 4$ and 5 and a nonlinear least squares fit was applied to the parallel plate cavity dispersion equation:

$$\tilde{\nu}_{cavity} = \frac{1}{2\pi}\left(\frac{n_b}{n_2}\right)\sqrt{\left(\frac{m\pi}{n_b d}\right)^2 + k_x^2} \quad , \quad (3)$$

where n_2 is the refractive index of the dielectric in the cavity, n_b is the refractive index outside of the cavity (air, note that the etalon may be mounted on a substrate or submerged in a different dielectric), m is the mode of the cavity fringe, d is the thickness of the cavity, and $k_x = 2\pi\tilde{\nu}sin\theta$, where θ is angle between the surface normal and incoming light wavevector (see Figure 1 inset). The input of $\tilde{\nu}_{cavity}$ and θ for each transmission max position of fringes $m = 4$ and 5 was used with Matlab's "fitnlm" toolbox function to obtain optimized fit parameters of

$n_2 = 1.368(7)$ and $d = 10.57(6)\ \mu m$ with errors in parenthesis in the least significant digit. These constants are used to predict the position of the $m = 3$ fringe in the absence of interaction with the vibration.

The position of the vibration in the absence of cavity modes is shown with a solid red line and the predicted position of the cavity fringe is shown with a solid green line. There is a crossover at $k_x \sim 230\ cm^{-1}$ or $\theta = 2^o$ at which point the Rabi splitting can be observed to be ~40 cm^{-1}. The mixed states, $\tilde{E}_i$, were measured as maxima in the transmission and are presented as cyan symbols in Figure 2. Both the upper and lower branches were fit together with the real part of the eigenvalues, $\Re(\lambda)$, of a $2x2$ model Hamiltonian[23-24]

$$\begin{vmatrix} \tilde{\nu}_{vib} - i\tilde{\gamma}_{vib} - \lambda & \tilde{V} \\ \tilde{V} & \tilde{\nu}_{cav} - i\tilde{\gamma}_{cav} - \lambda \end{vmatrix} = 0 \quad , \quad (4)$$

where a Matlab program decided the appropriate eigenvalue for the upper and lower branches using a flag for the branch. The diagonal elements were $\tilde{\nu}_{vib} - i\tilde{\gamma}_{vib} = 1037.9\ cm^{-1} - i11.2\ cm^{-1}$ from the vibration not in a cavity and $\tilde{\nu}_{cav} - i\tilde{\gamma}_{cav}$ with $\tilde{\nu}_{cav}$ from the $m = 3$ fringe

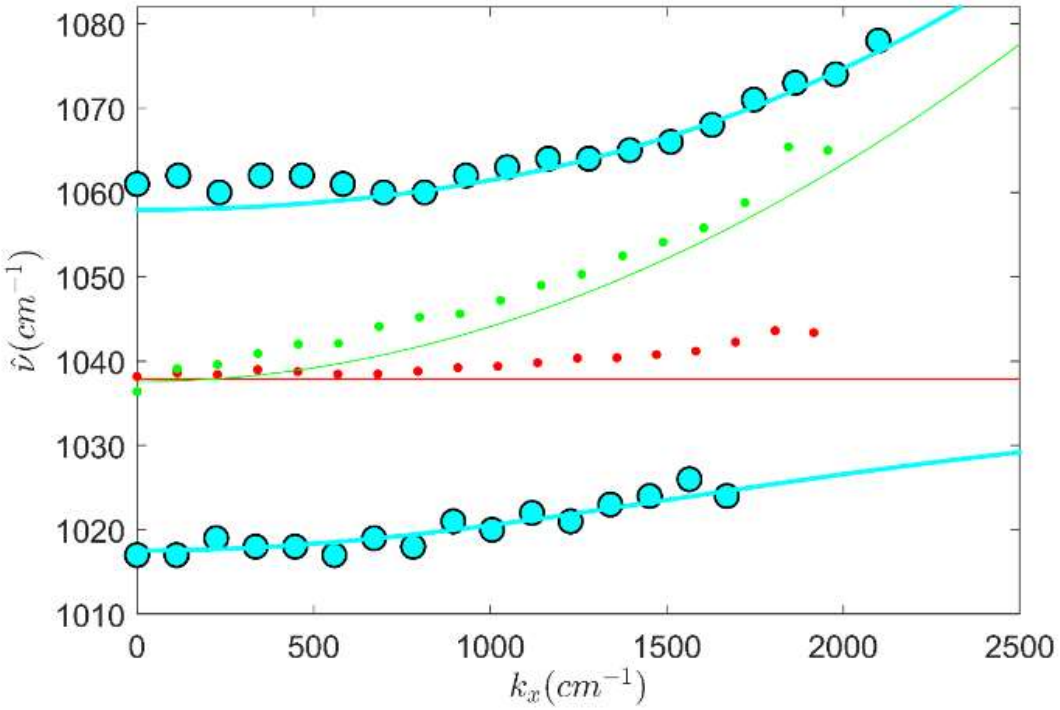

Figure 2. Rabi splitting measurement for CD_3 deformation vibration of $CD_3C{\equiv}N$ interacting with the $m = 3$ fringe of the cavity. The larger cyan symbols show the measured peak positions of the mixed states and the cyan curves are a fitted model of the cavity-vibration interaction. The solid red and greencurves show the noninteracting positions of the vibration (red),from a measured spectrum of $CD_3C{\equiv}N$ and the fringe (green), from equation 3 using fit values for n and d. The recovered bulk vibration and fringe positions are shown with red and green symbols, respectively, which show discernible shifts.

position of equation 3 and $\tilde{\gamma}_{cav} = 21.9\ cm^{-1}$ where the $\tilde{\nu}$ are peak positions and the $\tilde{\gamma}$ are half-width-at-half-maxima (HWHM). The off-diagonal cavity-vibration coupling element is $\tilde{V}$. The best fit value of $\tilde{V}$ was used to obtain the cyan solid lines in Figure 2. A standard deviation $\sigma_y = 1.2\ cm^{-1}$ of comparison between the fitted eigenvalues and $\tilde{E}_i$ transmission maxima in Figure 2 was used to estimate the errors in the $\tilde{V}$ coupling parameter as

$$\Delta V = \sigma_y \sqrt{\frac{1}{\sum_i (\Delta\tilde{E}/\Delta\tilde{V})_i^2}} \quad , \qquad (6)$$

where $(\Delta\tilde{E}/\Delta\tilde{V})_i$ was determined numerically at each point with $\pm$0.5% deviations from the best fit value of $\tilde{V}$. The run in Figure 2 yielded $\tilde{V} = 21.54 \pm 0.20\ cm^{-1}\ (esd)$ using $n_2 = 1.3675$ and $d = 10.572\ \mu m$. Two other runs with different nominally 12 μm spacers obtained $\tilde{V} = 21.3 \pm 0.5\ cm^{-1}\ (esd)$ and $\tilde{V} = 21.7 \pm 0.4\ cm^{-1}\ (esd)$. Assuming $\tilde{V}$ is constant in this momentum space, our averaged result is $\tilde{V} = 21.5 \pm 0.7\ cm^{-1}$ (95% $confidence, N = 3$). Fringe widths are known[1-2] to affect the "observed" Rabi splitting at the crossover approximately as

$$\tilde{\nu}_{1,0}(cm^{-1}) = 2\sqrt{\tilde{V}^2 - \left(\frac{\tilde{\gamma}_{vib} - \tilde{\gamma}_{cav}}{2}\right)^2}\ . \qquad (7)$$

If $(\tilde{\gamma}_{vib} - \tilde{\gamma}_{cav})/2 = 0\ cm^{-1}$, then the Rabi splitting is just $\tilde{\nu}_{1,0}(cm^{-1}) = 2\tilde{V} = 43.0 \pm 1.4\ cm^{-1}$. However, in the case of Figure 2, $(\tilde{\gamma}_{vib} - \tilde{\gamma}_{cav})/2 = 5.4\ cm^{-1}$ and a value of $\tilde{\nu}_{1,0}(cm^{-1}) = 41.6\ cm^{-1}$ was observed. Clearly, it is desirable to have the fringe width match the vibration width[16].

The next results involve fitting the bulk vibrational features. Since the fringe is about a factor of 2 wider than the vibration, the fringe was reconstructed using regions away from the narrower vibration at each and every angle θ. Measured transmission spectra, s_i, are shown with symbols in Figure 3a at six selected angles. The heavier symbols at each end of the range were fit to a quartic polynomial using Matlab's "polyfit" function as shown with solid lines in Figure 3a, i.e. avoiding the vibrational feature. The max position of the fringe was inferred from the max of the fitted polynomial as shown with an open red symbol in Figure 3a revealing that the fringe is being angle-tuned through the vibration. Finally, the fitted fringe polynomial was used

as a transmission background, b_i, for the measured vibrational transmission data, s_i, to obtain an extinction vibrational lineshape, i.e. $-log(s_i/b_i)$ as shown in Figure 3b with symbols. The lineshapes were all dominated by absorption and close to Lorentzian shapes, but there can also be dispersive characteristics in thin film spectra[25], so each was fit to an absorption/dispersion lineshape[25-27] (solid lines in Figure 3b) as

$$I(\tilde{\nu}) = \frac{\frac{S}{\Gamma}\left[cos\varphi - \left(\frac{\tilde{\nu}-\tilde{\nu}_0}{\Gamma}\right)sin\varphi\right]}{1+\left(\frac{\tilde{\nu}-\tilde{\nu}_0}{\Gamma}\right)^2} + c\,, \qquad (8)$$

where φ is the phase shift, S is the linestrength, $\tilde{\nu}_0$ is the transition position $(1/\lambda)$, and Γ is the half-width-at-half-max (HWHM). If the

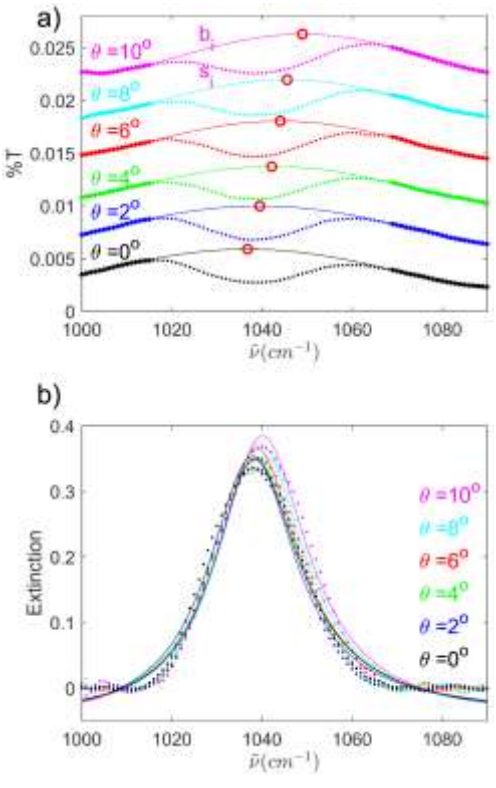

Figure 3. a) Reconstruction of fringe (solid line, b_i) with quartic polynomial fit using regions away from vibration (larger symbols). Red circles show the fringe maximum in the absence of a vibration. Colored points, s_i, are measured data. Offsets were used to visually separate transmission spectra. b) Use of the reconstructed fringe as a background for an extinction lineshapeof bulk vibrations which make small but statistically meaningful changes. Solid curves are equation 8 and points are $-log(s_i/b_i)$.

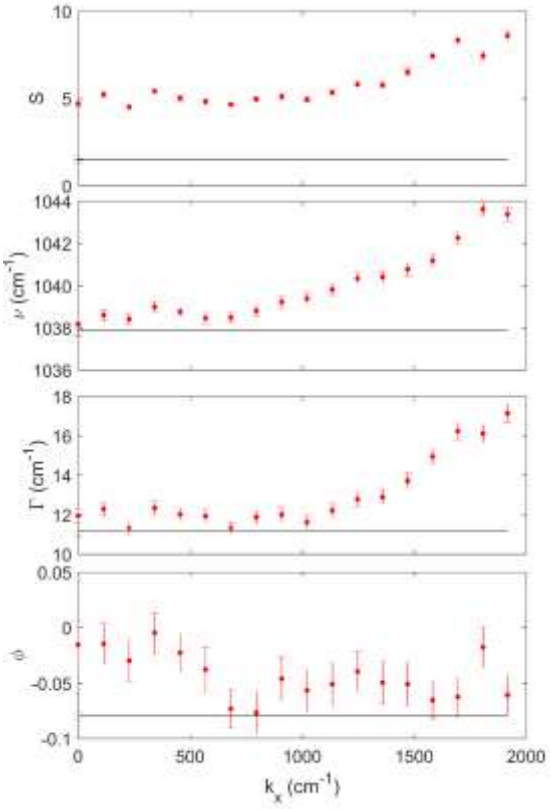

Figure 4. Plot of bulk vibrational lineshape parameters S (linestrength), $\tilde{\nu}$ (peak position), Γ (half-width-at-half-max), and ϕ (phase in radians) vs wavevector as affected by being in a cavity. The vibrational parameters without a cavity are shown in black. Errorbars are the standard errors upon fitting to eq. (5).

phase shift is zero, then only the cos φ term survives and the form is pure Lorentzian for absorption. Thin films are notorious for such phase changes and this form was essential for the extraction of meaningful results. Many of the absorption/dispersion lineshape fit parameters of the bulk vibrations are shown in Figure 4 which includes error bars to show that the changes are significant relative to random errors. The phase φ in Equation 8 has fitted values in a range from 0 to -0.1 radians (0 to -6°), so the lineshapes are not pure absorption, but close, i.e. dominated by absorption. Dispersion was small but detectable by non-zero values of φ. There are dramatic differences from measurement without a cavity and changes as the system departs from the cavity-vibration crossover point. The bulk vibrational linestrength starts at 5 and increases to ~8, the bulk vibrational frequency changes from 1038 to 1044 cm^{-1}, and the bulk linewidths increase from 12 to 17 cm^{-1} over the wavevector range. Such changes in the bulk vibrational frequency imply that there was a ~1% increase in the vibrational force constant due to being inside the cavity. The increase in bulk vibrational width may indicate a shortening of bulk vibrational lifetime in the resonant cavity.

CONCLUSIONS

It is interesting to consider these results in terms of the photon (n) and vibrational oscillator (N) numbers within the cavity[28]. Assuming 5 W of power inside the cavity with multipassing (an overestimate) leads to $n < 10^7$ photons. Likewise, a crude estimate of the number of vibrational oscillators assuming a 3 mm effective spot radius for the Gaussian illuminated cavity is $\sim 4x10^{18}$. There are something like 11 orders of magnitude more vibrational oscillators than photons in the experimental cavity. If it takes one photon and one vibration to make a dressed state, the dressed states are a negligible fraction of the vibrational

oscillators within the cavity. In spite of this, the major conclusion is that the bulk vibrational signals are affected as shown in Figure 4.

There is the question of whether our results pertain to the "dark" states of cavity-vibration coupling[17, 29-31], but there seem to be different meanings for dark states. Some describe dark states as weakly absorbing polaritons or collective states with harmonically forbidden intensity from the ground state[17, 29-30] and these are likely obscured in our results. However, others[31] discuss an incoherent manifold and effects of inhomogeneity[31] and there may be a connection to our results from this perspective. To avoid this confusion, "bulk vibrational states" is used in this work. The method displayed in Figure 3 is one that a molecular spectroscopist would use to detect a spectral signature using enhancement by multipassing in an etalon. Spectroscopists would start with the assumption that the interaction with light inside the cavity is weak and that the lineshape is unperturbed from that outside of a cavity. Our assumption is that experimental conditions of this work reside in a region where strong coupling begins, but is not strong enough to wipe out all transmission in the region of the bulk vibrational absorption. Hence, the beginning of strong coupling effects are observed in the bulk vibrational lineshapes.

It is now known that cavity-vibration[32] and cavity-electronic[33-34] interactions can slow the rate of chemical reactions. The question arises as to the role of dressed states vs bulk vibrations in these kinetics. It will be interesting to track and correlate the bulk vibrational changes with kinetic results in cavities, as well as to change the experimental configurations to make dressed states more prominent.

Finally, the comparison of traditional IR intensity measurements to theory is difficult because it involves integrating or summing transition intensities over carefully controlled

conditions and well-understood partition functions and the use of highly correlated wave functions[35] on the theory side. Since cavity-vibration Rabi splittings lie in frequency space, there may be advantages in measuring energy splittings regarding the comparison to fundamental properties like mass weighted dipole derivatives (see Equation 2) facilitating easier comparison between experiment and theory.

AUTHOR INFORMATION

Corresponding Author:

* coe.1@osu.edu

The authors declare no competing financial interests.

ACKNOWLEDGMENT

We gratefully acknowledge the National Science Foundation for support of this work under grant number CHE 1800414.

REFERENCES

(1) Long, J. P.; Simpkins, B. S., Coherent Coupling between a Molecular Vibration and Fabry-Perot Optical Cavity to Give Hybridized States in the Strong Coupling Limit. *ACS Photonics* **2015,** *2* (1), 130-136.

(2) Simpkins, B. S.; Fears, K. P.; Dressick, W. J.; Spann, B. T.; Dunkelberger, A. D.; Owrutsky, J. C., Spanning Strong to Weak Normal Mode Coupling between Vibrational and Fabry-Perot Cavity Modes through Tuning of Vibrational Absorption Strength. *ACS Photonics* **2015,** *2* (10), 1460-1467.

(3) Shalabney, A.; George, J.; Hutchison, J.; Pupillo, G.; Genet, C.; Ebbesen, T. W., Coherent coupling of molecular resonators with a microcavity mode. *Nat. Commun.* **2015,** *6*, 5981.

(4) Shalabney, A.; George, J.; Hiura, H.; Hutchison, J. A.; Genet, C.; Hellwig, P.; Ebbesen, T. W., Enhanced Raman Scattering from Vibro-Polariton Hybrid States. *Angew. Chem., Int. Ed.* **2015,** *54* (27), 7971-7975.

(5) George, J.; Shalabney, A.; Hutchison, J. A.; Genet, C.; Ebbesen, T. W., Liquid-Phase Vibrational Strong Coupling. *Journal of Physical Chemistry Letters* **2015,** *6* (6), 1027-1031.

(6) Thomas, A.; George, J.; Shalabney, A.; Dryzhakov, M.; Varma, S. J.; Moran, J.; Chervy, T.; Zhong, X.; Devaux, E.; Genet, C.; Hutchison, J. A.; Ebbesen, T. W., Ground-State Chemical Reactivity under Vibrational Coupling to the Vacuum Electromagnetic Field. *Angew. Chem. Int. Ed.* **2017,** *55*, 11462-11466.

(7) Vergauwe, R. M. A.; George, J.; Chervy, T.; Hutchison, J. A.; Shalabney, A.; Torbeev, V. Y.; Ebbesen, T. W., Quantum Strong Coupling with Protein Vibrational Modes. *J. Phys. Chem. Lett.* **2016,** *7* (20), 4159-4164.

(8) Kapon, O.; Muallem, M.; Palatnik, A.; Aviv, H.; Tischler, Y. R., A simplified method for generating periodic nanostructures by interference lithography without the use of an anti-reflection coating. *Appl. Phys. Lett.* **2015,** *107* (20), 201105/1-201105/5.

(9) Muallem, M.; Palatnik, A.; Nessim, G. D.; Tischler, Y. R., Strong Light-Matter Coupling and Hybridization of Molecular Vibrations in a Low-Loss Infrared Microcavity. *J. Phys. Chem. Lett.* **2016,** *7* (11), 2002-2008.

(10) Muallem, M.; Palatnik, A.; Nessim, G. D.; Tischler, Y. R., Strong light-matter coupling between a molecular vibrational mode in a PMMA film and a low-loss mid-IR microcavity. *Ann. Phys. (Berlin, Ger.)* **2016,** *528* (3-4), 313-320.

(11) Ahn, W.; Vurgaftman, I.; Dunkelberger, A. D.; Owrutsky, J. C.; Simpkins, B. S., Vibrational Strong Coupling Controlled by Spatial Distribution of Molecules within the Optical Cavity. *ACS Photonics* **2017**.

(12) Casey, S. R.; Sparks, J. R., Vibrational Strong Coupling of Organometallic Complexes. *J. Phys. Chem. C* **2016,** *120* (49), 28138-28143.

(13) Crum, V. F.; Casey, S. R.; Sparks, J. R., Photon-mediated hybridization of molecular vibrational states. *Phys. Chem. Chem. Phys.* **2018,** *20* (2), 850-857.

(14) Chervy, T.; Thomas, A.; Akiki, E.; Vergauwe, R. M. A.; Shalabney, A.; George, J.; Devaux, E.; Hutchison, J. A.; Genet, C.; Ebbesen, T. W., Vibro-Polaritonic IR Emission in the Strong Coupling Regime. *ACS Photonics* **2018,** *5* (1), 217-224.

(15) Dunkelberger, A. D.; Davidson Ii, R. B.; Ahn, W.; Simpkins, B. S.; Owrutsky, J. C., Ultrafast Transmission Modulation and Recovery via Vibrational Strong Coupling. *J. Phys. Chem. A* **2018,** *122* (4), 965-971.

(16) Kapon, O.; Yitzhari, R.; Palatnik, A.; Tischler, Y. R., Vibrational Strong Light-Matter Coupling Using a Wavelength-Tunable Mid-infrared Open Microcavity. *J. Phys. Chem. C* **2017,** *121* (34), 18845-18853.

(17) Ebbesen, T. W., Hybrid Light-Matter States in a Molecular and Material Science Perspective. *Acc. Chem. Res.* **2016,** *49* (11), 2403-2412.

(18) Torma, P.; Barnes, W. L., Strong coupling between surface plasmon polaritons and emitters: a review. *Rep. Prog. Phys.* **2015,** *75*, 013901/1-013901/34.

(19) Haroche, S.; Kleppner, D., CAVITY QUANTUM ELECTRODYNAMICS. *Phys. Today* **1989,** *42* (1), 24-30.

(20) M. J. Frisch, G. W. T., H. B. Schlegel, G. E. Scuseria, ; M. A. Robb, J. R. C., J. A. Montgomery, Jr., T. Vreven, ; K. N. Kudin, J. C. B., J. M. Millam, S. S. Iyengar, J. Tomasi, ; V. Barone, B. M., M. Cossi, G. Scalmani, N. Rega, ; G. A. Petersson, H. N., M. Hada, M. Ehara, K. Toyota, ; R. Fukuda, J. H., M. Ishida, T. Nakajima, Y. Honda, O. Kitao, ; H. Nakai, M. K., X. Li, J. E. Knox, H. P. Hratchian, J. B. Cross, ; C. Adamo, J. J., R. Gomperts, R. E. Stratmann, O. Yazyev, ; A. J. Austin, R. C., C. Pomelli, J. W. Ochterski, P. Y. Ayala, ; K. Morokuma, G. A. V., P. Salvador, J. J. Dannenberg, ; V. G. Zakrzewski, S. D., A. D. Daniels, M. C. Strain, ; O. Farkas, D. K. M., A. D. Rabuck, K. Raghavachari, ; J. B. Foresman, J. V. O., Q. Cui, A. G. Baboul, S. Clifford, ; J. Cioslowski, B. B. S., G. Liu, A. Liashenko, P. Piskorz, ; I. Komaromi, R. L. M., D. J. Fox, T. Keith, M. A. Al-Laham, ; C. Y. Peng, A. N., M. Challacombe, P. M. W. Gill, ; B. Johnson, W. C., M. W. Wong, C. Gonzalez, and J. A. Pople, *Gaussian 03*, Revision B.04; Gaussian, Inc., Pittsburgh PA: 2003.

(21) Swanton, D. J.; Bacskay, G. B.; Hush, N. S., An ab initio SCF calculation of the dipole-moment derivatives and infrared-absorption intensities of the water-dimer molecule. *Chem. Phys.* **1983,** *82* (3), 303-15.

(22) Swanton, D. J.; Bacskay, G. B.; Hush, N. S., A quantum chemical study of the infrared absorption intensities of the isoelectronic C3v systems ammonia, protonated water cation (H3O+) and methyl(1-). *Chem. Phys.* **1986,** *107* (1), 9-23.

(23) Panzarini, G.; Andreani, L. C.; Armitage, A.; Baxter, D.; Skolnick, M. S.; Astratov, V. N.; Roberts, J. S.; Kavokin, A. V.; Vladimirova, M. R.; Kaliteevski, M. A., Exciton-light coupling in single and coupled semiconductor microcavities: Polariton dispersion and polarization splitting. *Phys. Rev. B: Condens. Matter Mater. Phys.* **1999,** *59* (7), 5082-5089.

(24) Savona, V.; Andreani, L. C.; Schwendimann, P.; Quattropani, A., Quantum well excitons in semiconductor microcavities: unified treatment of weak and strong coupling regimes. *Solid State Commun.* **1995,** *93* (9), 733-9.

(25) Ravi, A.; Malone, M. A.; Luthra, A.; Lioi, D.; Coe, J. V., Spectral challenges of individual wavelength-scale particles: strong phonons and their distorted lineshapes. *PCCP* **2013,** *15* (25), 10307-10315.

(26) Marshall, A. G.; Roe, D. C., Dispersion versus absorption: spectral line shape analysis for radiofrequency and microwave spectrometry. *Anal. Chem.* **1978,** *50* (6), 756-63.

(27) Bruce, R. E.; Marshall, A. G., Linearized dispersion:absorption plots for spectral line-shape analysis. *J. Phys. Chem.* **1980,** *84* (11), 1372-5.

(28) Haroche, S.; Raimond, J.-M., *Exploring the Quantum: Atoms, Cavities, aaand Photons*. Oxford: 2013; p 616.

(29) Houdre, R.; Stanley, R. P.; Ilegems, M., Vacuum-field Rabi splitting in the presence of inhomogeneous broadening: resolution of a homogeneous linewidth in an inhomogeneously broadened system. *Phys. Rev. A: At., Mol., Opt. Phys.* **1996,** *53* (4), 2711-15.

(30) Herrera, F.; Spano, F. C., Dark vibronic polaritons and the spectroscopy of organic microcavities. *Phys. Rev. Lett.* **2017,** *118* (22), 223601/1-223601/6.

(31) Ribeiro, R. F.; Martinez-Martinez, L. A.; Du, M.; Campos-Gonzalez-Angulo, J.; Yuen-Zhou, J., Polariton chemistry: controlling molecular dynamics with optical cavities. *Chem. Sci.* **2018,** *9* (30), 6325-6339.

(32) Thomas, A.; George, J.; Shalabney, A.; Dryzhakov, M.; Varma, S. J.; Moran, J.; Chervy, T.; Zhong, X.; Devaux, E.; Genet, C.; Hutchison, J. A.; Ebbesen, T. W., Ground-State Chemical Reactivity under Vibrational Coupling to the Vacuum Electromagnetic Field. *Angew. Chem., Int. Ed.* **2016,** *55* (38), 11462-11466.

(33) Zhong, X.; Chervy, T.; Wang, S.; George, J.; Thomas, A.; Hutchison, J. A.; Devaux, E.; Genet, C.; Ebbesen, T. W., Non-Radiative Energy Transfer Mediated by Hybrid Light-Matter States. *Angew. Chem., Int. Ed.* **2016,** *55* (21), 6202-6206.

(34) Hutchison, J. A.; Schwartz, T.; Genet, C.; Devaux, E.; Ebbesen, T. W., Modifying Chemical Landscapes by Coupling to Vacuum Fields. *Angew. Chem.-Int. Edit.* **2012,** *51* (7), 1592-1596.

(35) Galabov, B.; Yamaguchi, Y.; Remington, R. B.; Schaefer, H. F., III, High Level ab Initio Quantum Mechanical Predictions of Infrared Intensities. *J. Phys. Chem. A* **2002,** *106* (5), 819-832.